Biochemical and Biophysical Research Communications 377 (2008) 146–150

Contents lists available at ScienceDirect

Biochemical and Biophysical Research Communications

journal homepage: www.elsevier.com/locate/ybbrc

DE loop mutations affect β2-microglobulin stability and amyloid aggregation

Stefano Ricagno [a], Matteo Colombo [a], Matteo de Rosa [a,1], Enrico Sangiovanni [a], Sofia Giorgetti [b,c], Sara Raimondi [b,c], Vittorio Bellotti [b,c], Martino Bolognesi [a,*]

[a] Department of Biomolecular Sciences and Biotechnology, CNR-INFM and CIMAINA, University of Milano, Via Celoria 26, 20133 Milano, Italy
[b] Department of Biochemistry, University of Pavia, Via Taramelli 3/b, 27100 Pavia, Italy
[c] Laboratories of Biotechnology IRCCS, Fondazione Policlinico San Matteo, 27100 Pavia, Italy

ARTICLE INFO

Article history:
Received 17 September 2008
Available online 1 October 2008

Keywords:
β2-Microglobulin
Amyloid fibrils
Dialysis-related amyloidosis
Protein X-ray structure
Protein thermal stability

ABSTRACT

β2-Microglobulin (β2m) is the light chain component of class I major histocompatibility complex (MHC-I). β2m is an intrinsically amyloidogenic protein that can assemble into amyloid fibrils *in vitro* and *in vivo*. Several recent reports suggested that the polypeptide loop comprised between β-strands D and E of β2m is important for protein stability and for the protein propensity to aggregate as amyloid fibrils. In particular, the roles of Trp60 for MHC-I assembly and β2m stability have been highlighted by showing that the β2m Trp60 → Gly mutant is more stable and less prone to aggregation than the wild type protein. To further analyse such properties, the Trp60 → Cys and Asp59 → Pro β2m mutants have been expressed, purified, and their crystal structures determined. The stability to thermal denaturation and propensity to fibrillar aggregation have also been analysed. The experimental evidences gathered on the two mutants reinforce the hypothesis that conformational strain in the DE loop can affect β2m stability and amyloid aggregation properties.

In vivo fibrillar protein aggregation, often referred to as amyloid aggregation, has gained wide interest, being at the basis of several degenerative diseases such as Alzheimer in man or spongiform encephalopathy in cows [1]. Formation of amyloid precipitate arises from the aggregation of misfolded protein molecules into elongated protein fibrils, known as cross-β or amyloid fibrils. However the molecular details of fibril formation are only marginally understood. It is generally recognized that during fibrillation protein molecules loose their native fold, increase their β secondary structure content, and, via intermolecular β-strand interactions, the misfolded protein molecules polymerise into elongated amyloid fibrils. The cross-β assembly (named after a typically recurring X-ray fibre diffraction pattern) [2,3] is very stable, such that amyloid fibrils are very resistant mechanically and to chemical degradation [1]. *In vivo* fibrils accumulate and, being resistant to proteolysis, they can deposit in large amounts in different tissues [1].

β2-Microglobulin (β2m) is a 99 amino acid protein, which constitutes the light chain of the class I major histocompatibility complex (MHC-I) and of CD1 [4]. β2m has the typical immunoglobin β-sandwich fold, consisting of seven β-strands organised in two β-sheets linked by a disulphide bond [5]. Kidneys are responsible for β2m degradation in the human body. Patients with kidney failure regularly undergo hemodialysis treatments, which in the long term result in the accumulation of free β2m in the blood, up to concentrations 20–30 times higher than the physiological level. This condition facilitates β2m aggregation into fibrils and leads to dialysis-related amyloidosis (DRA), a pathology characterized by β2m amyloid aggregation and deposit in skeletal joints, seriously affecting their functionality [6].

Although several studies on β2m aggregation are available, the molecular mechanism underlying cross-β fibril formation has yet to be properly understood. Full length β2m can be converted *in vitro* into amyloid fibrils under various experimental conditions, including low and neutral pH [7]. The use of 20% trifluoroethanol (TFE), at neutral pH, is a particularly efficient procedure in terms of fibril formation rate and yield. Analysis of the amyloid plaques extracted from DRA patients shows that full length β2m is the major component of the fibrils, while a truncated form of β2m lacking six amino acids at the N-*terminus* makes up about 20–30% of the aggregated material [8,9].

Over the past few years numerous efforts have been focused on studying the structural bases and mechanisms of β2m fibril formation, since β2m is regarded as a molecular model for folding and for the amyloid transition process (for review Chatani and Goto 2005) [10]. Increasing attention has been focussed on β2m residue Trp60

Abbreviations: w.t., wild type; β2m, β2-microglobulin; W60C, β2-microglobulin Trp60 → Cys mutant; D59P, β2-microglobulin Asp59 → Pro mutant; W60G, β2-microglobulin Trp60 → Gly mutant; MHC-I, class I major histocompatibility complex; TFE, trifluoroethanol; DRA, dialysis-related amyloidosis.

* Corresponding author. Fax: +39 02 50314895.
E-mail address: martino.bolognesi@unimi.it (M. Bolognesi).
[1] Present address: Instituto de Tecnologia Quimica e Biologica, Universidade Nova de Lisboa, Avenue da Republica, 2780-157 Lisbon, Portugal.

0006-291X/$ - see front matter © 2008 Elsevier Inc. All rights reserved.
doi:10.1016/j.bbrc.2008.09.108

that plays a key role in fibrillogenesis [11]. It is exposed in the native β2m fold, and NMR H/D exchange experiments show that it is solvent accessible in the fibrils [12]. In a recent report, Trp60 was substituted by Gly (W60G), showing that this β2m mutant is more stable to unfolding than the w.t. protein and is not fibrillogenic under mild conditions [13]. It was proposed that W60G higher stability may partly result from a geometrical relaxation of the DE loop, relative to the w.t. protein, suggesting that removal of the bulky hydrophobic Trp side chain may also increase the solubility of isolated β2m and decrease its tendency to aggregation [13].

In order to characterise more deeply the role of geometric strain and hydrophobicity in the β2m DE loop, here we report the production and biophysical characterisation of two β2m mutants, W60C and D59P. The Trp60 → Cys substitution maintains the same DE loop backbone stereochemical restraints of the w.t. protein, while removing the bulky Trp side chain. On the other hand, the Asp59 → Pro mutation was designed in order to increase the rigidity of the DE loop. The crystal structures of the W60C and D59P mutants are here reported together with an analysis of their thermal stability and their propensity for amyloid aggregation.

Materials and methods

Mutants preparation & purification. Mutagenesis of Trp60 into Cys, and of Asp59 into Pro were carried out as in Esposito et al. [13]. The β2m mutants were subsequently expressed and purified as previously reported [13].

Crystallisation and structure determination. β2m D59P and W60C mutants were crystallised under the same conditions used for β2m W60G [13]. X-ray diffraction data collections were performed using the crystallization mother liquor as cryoprotectant at beam line ID14-2, at 100 K (ESRF, Grenoble). Diffraction data were processed using MOSFLM and SCALA [14,15]. β2m D59P and W60C structure solutions were achieved by molecular replacement, using PHASER [16] and the β2m W60G mutant atomic coordinates (PDB entry 2Z9T) as search model. Both structures were then refined with REFMAC5, with restrained and 'tls' refinement methods [17]. Model building and structure analysis was performed with COOT [18]. Coot was also used to calculate Ramachandran and Kleywegt plots. Fig. 1 has been prepared using Pymol (http://pymol.sourceforge.net). Atomic coordinates and structure factors for the β2m D59P and W60C structures have been deposited with the Protein Data Bank, with accession codes 3DHJ and 3DHM, respectively.

Thermal stability. The thermal stability of β2m mutants was assessed by thermofluorescence analysis using a protocol similar to that described in Ericsson et al. [19] A MJ MINI real time PCR apparatus (BIORAD) equipped with MiniOpticon was used to carry out thermal unfolding, and monitored by Sypro Orange fluorescence signal (465 and 590 nm for excitation and emission wavelengths, respectively). Protein samples in water at a final concentration of 2 mg/ml were tested in the 30–80 °C temperature range.

Amyloid fibril formation. pH 7.4 procedure: 100 μM β2 m was incubated at 37 °C in 50 mM Na phosphate buffer, 100 mM NaCl, pH 7.4, in the presence of 20% (v/v) TFE [20]. 20 μg/ml of β2m fibril seeds were added to the samples. pH 2.5 procedure: 100 μM β2m was incubated at 37 °C in 50 mM Na-citrate, 100 mM NaCl, pH 2.5, in the presence of 20 μg/ml of β2 m fibril seeds [21]. Amyloid formation was quantitatively assessed using Thioflavin T (ThT), according to LeVine [22]. ThT (SIGMA) concentration was 10 μM, in 50 mM glycine/NaOH buffer, pH 8.5. Fluorescence measurements were carried out by excitation at 445 nm, and emission collected at 485 nm. The fibrillogenesis of w.t. β2 m and the mutants W60C and D59P were followed by ThT fluorescence, which is reported in arbitrary units. The ThT fluorescence values were measured after 3 days of incubation at 37 °C.

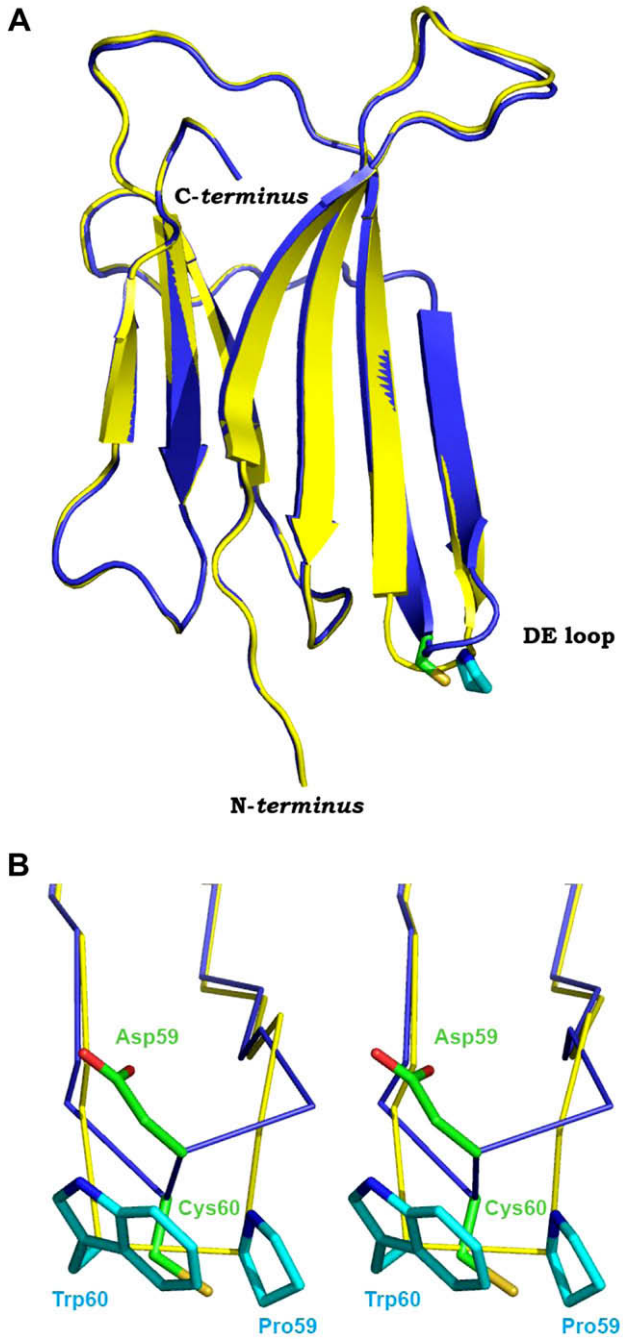

Fig. 1. Mutation of residues in the DE loop of β2m. (A) Ribbon representation of the two superposed β2m mutants: W60C is colored in blue and D59P is in yellow. Pro59 and Cys60 mutated residues are shown as stick models in the lower part of the figure. (B) Superposition of W60C and D59P DE loops (stereo view), color coded as in A. Stick representation of residues 59 and 60 is shown in green for W60C and cyan for D59P. (For interpretation of the references to color in this figure legend, the reader is referred to the web version of this paper.)

Results

Crystal structures of β2m Trp60Cys and Asp59Pro mutants

The structure of the W60C mutant was solved and refined at 2.0 Å resolution, with R-gen and R-free values of 17.3% and 21.2%, respectively (see Table 1). The overall W60C structure matches closely that of W60G (PDB entry 2Z9T), which was used as search model (Fig. 1A): the RMSD is 0.18 Å over 99 Cα atom

Table 1
Data collection and refinement statistics for the β2m W60C and D59P mutants

	β2m W60C	β2m D59P
Beam line	ESRF ID14-2	ESRF ID14-2
Space group	Monoclinic C2	Monoclinic C2
Unit cell edges (Å, °)	a = 77.35 b = 28.87 c = 64.79 β = 132.5°	a = 78.18 b = 29.19 c = 55.32 β = 121.4°
Resolution (Å)	20–2.0	20–1.80
R merge[a] (%)	11.2 (42.0)	11.3 (42.1)
$I/\sigma I$	9.7 (2.5)	12.2 (2.4)
Completeness (%)	94.8 (94.8)	94.9 (94.9)
Redundancy	5.0 (3.8)	5.0 (3.8)
Unique reflections	7339	10110
Refinement		
R work[b] (%)	17.3	18.9
R-free (%)	21.2	22.2
Number of atoms		
Protein	845	836
Water	74	70
Ramachandran plot		
Most favoured region	97%	98%
Allowed region	3%	1%
Outliers	0%	1%

Values in parenthesis are for the highest resolution shell.
[a] R merge = $\Sigma|I - \langle I\rangle|/\Sigma|I|$ where I is the observed intensity and $\langle I\rangle$ is the average intensity.
[b] R work = $\Sigma_{hkl}||F_o| - |F_c||/\Sigma_{hkl}|F_o|$ for all data except 5% which were used for R-free calculation.

pairs. Both structures show the same conformation of the DE loop, where the Gly60 and Cys60 mutations lie. Conversely, structural comparison between W60C and the isolated w.t. β2m chain (PDB entry 1LDS) [23] shows an RMSD of 0.58 Å, calculated over all 97 Cα atoms of the w.t. structure; a different conformation of the DE loop is mainly responsible for the higher RMSD. Thus, in the Ramachandran plot of W60C the (φ, ψ) pair for Cys60 (65°, 5°) matches closely the value observed for Gly60 in the W60G structure, and for Trp60 in the β2m MHC-I complex (PDB entry 1BSS), but not that of Trp60 in the isolated w.t. β2m chain (−115°, 15°).

The structure of the D59P mutant was solved and refined at 1.8 Å resolution, with R-gen and R-free values of 18.9% and 22.2%, respectively (see Table 1). The structure of D59P appears to be mostly similar to w.t. β2m isolated chain (PDB entry 1LDS; RMSD of 0.19 Å over 97 Cα pairs), adopting the same conformation of the DE loop. On the other hand, the RMSD increases when the D59 P Cα backbone is superposed to W60G (PDB entry 2Z9T), and to W60C: 0.57 Å and 0.40 Å RMSD values, respectively (over 99 Cα pairs), due to different conformations of the DE loop (Fig. 1B). The Ramachandran plot of w.t. β2m (PDB entry 1LDS) and D59P are almost identical, both showing signs of DE loop conformational strain. In the D59P structure Ser57 falls marginally in a not-allowed region of the Ramachandran plot, as in w.t. β2m isolated chain, but unlike in W60G. Moreover, analysis of the peptide ω angles reveals a significant deviation (37°) from planarity for Pro59.

Thermal stability and amyloid fibril formation

The thermal stability of W60C and D59P was assessed measuring the variation of fluorescence intensity of the Sypro Orange dye over the 30–80 °C temperature range. When a protein unfolds the protein hydrophobic core becomes solvent accessible and Sypro Orange can interact with it; upon interaction with hydrophobic amino acids Sypro Orange fluorescence increases; thus, the dye fluorescence allows monitoring β2m unfolding. Under our experimental conditions the Tm for w.t. β2m, W60C and D59P were found to be 60.1, 59.8, and 52.0 °C, respectively (Fig. 2A).

The ability of W60C and D59P to form fibrils was analysed (see Table 2). W60C could be converted into fibrils with low yield at pH 7.4, while at pH 2.5 W60C fibril formation was quantitatively comparable to the w.t. protein. D59P, instead, showed a stronger tendency than w.t. β2m to form fibrils, both in terms of aggregation rate and final fibril yield. After 4 h, under both the conditions tested, D59P samples show heavy precipitate, while the w.t. solution is still clear and ThT fluorescence is negligible. Under both fibrillogenesis conditions values of ThT fluorescence for D59P are two- and four-fold higher than those of w.t. β2m, respectively. Furthermore, fibril formation is faster than for w.t. β2m, indicating that D59P has an intrinsic higher propensity to amyloid aggregation.

Oligomerisation state of W60C

In the W60C mutant a Cys residue was introduced on the surface of the protein in a position totally exposed to the solvent. SDS–PAGE analysis under non-reducing conditions was employed to assess the tendency of W60C to form disulphide bond stabilized dimers. Our results showed that dimer abundance varies between 30% and 90%, depending on the purification batch. As an example, Fig. 2B shows two distinct W60C purification batches that are about 90% and 40% dimeric; such variability likely arises during the 72 h refolding process in the absence of reducing agents. In fact, addition of any reducing agent during the refolding procedure hampers the formation of the internal Cys25-Cys80 disulphide bond, with large loss in the yield of properly folded W60C. Since during refolding the redox conditions are not easily controlled, variable monomer/dimer ratios can be expected in different protein preparations. For crystallogenesis, and for the thermal unfolding experiments shown in Fig. 2A, the same batch with a low dimeric fraction was used. Notably, different W60C batches, characterized by different amounts of the dimeric species, showed undistinguishable behaviour during fibrillogenesis and thermal unfolding, suggesting that monomeric and dimeric W60C molecules assemble equally well in the fibrils, and that thermal unfolding of individual W60C chains, and their Sypro Orange interaction, are little affected by the intermolecular disulphide bridge.

When Cys residues were introduced at different β2m sites (residues 20, 50 and 88) only a small fraction of the expressed proteins was found to dimerise through an intermolecular disulphide bridge, whereas the dimerisation of W60C is always significant. It is noteworthy that fibrils generated from W60C, with high yield at pH 2.5, and with low yield at pH 7.4, were composed of both the monomeric and the dimeric species, without any significant enrichment of one of the two species, relative to the starting solution (Fig. 2B–D). Such finding would suggest that the intermolecular pairing of DE loops promoted by formation of the S–S bond is perfectly compatible with the fibril structure.

The higher W60C propensity to dimerise through Cys60 is in keeping with previous studies on the mechanism of β2m oligomerisation by Fogolari et al. 2007 [24], who predicted through molecular dynamics simulations that the highest number of intermolecular contacts within the fibril was achieved by Trp60. Moreover, chemical cross-linking confirmed that the DE loop is involved in specific intermolecular interactions [25].

Conclusion

β2m DE loop mutant

Among numerous studies on biophysical properties of β2m, a recent report on the W60G mutant has shown that the Trp60 → Gly mutation unexpectedly increases the protein stability, while not affecting the loop flexibility as would be expected for a

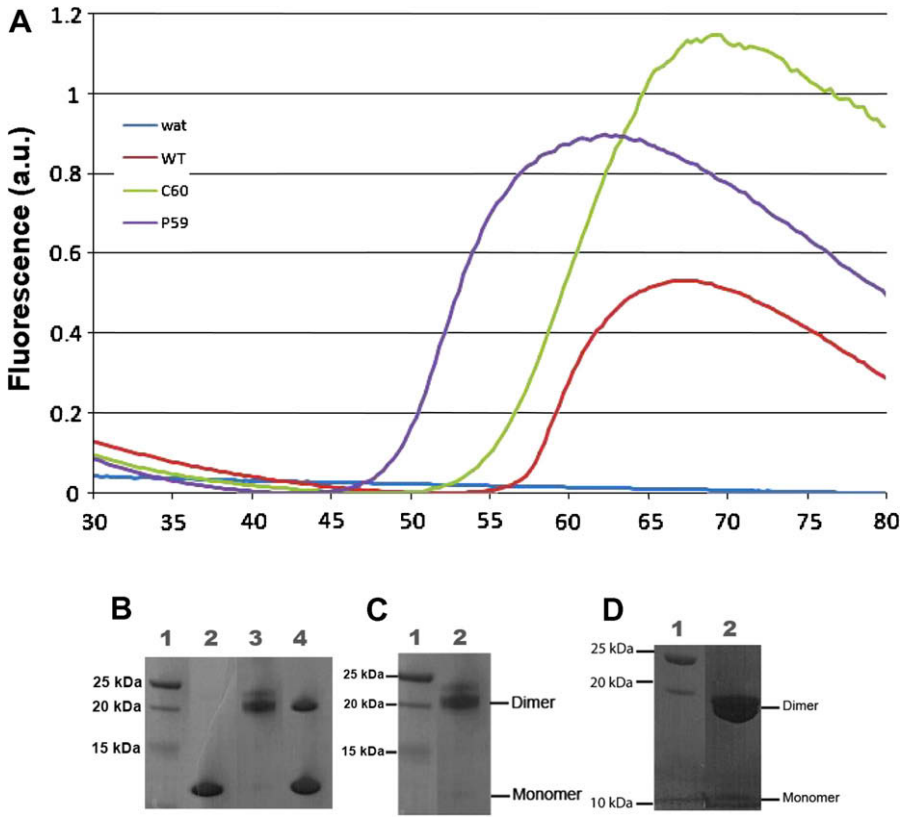

Fig. 2. (A) Thermal unfolding profiles monitored using Sypro Orange fluorescence: w.t. β2m in red, W60C in green and D59P in violet. SDS–PAGE under non-reducing conditions. (B) Lane 1, molecular weight standards; lane 2, w.t. β2m; lanes 3 and 4, two different W60C purification batches. The dimer content for the protein in lane 3 is about 90% of the total protein, while in lane 4 it is about 40%. (C) SDS–PAGE under non-reducing conditions of W60C showing (lane 2) a 90–10% distribution of dimer-monomer. This sample has been later used to perform fibrillogenesis experiments (see panel D). (D) SDS–PAGE under non-reducing conditions of W60C fibrils grown at pH 2.5 (lane 2). The fibrils were washed prior solubilisation in SDS buffer. The solubilised fibrils show the same dimer/monomer distribution observed in solution, reported in panel C. (For interpretation of the references to color in this figure legend, the reader is referred to the web version of this paper.)

Table 2
β2m w.t. and mutants amyloid fibril formation at pH 7.4 and pH 2.5 (ThT fluorescence)

	Fibrillogenesis pH 7.4	Fibrillogenesis pH 2.5
WT β2m	101 ± 12	121 ± 7
W60C	36 ± 8	95 ± 17
D59P	213 ± 23	420 ± 50

Gly containing region; moreover, it has been shown that W60G does not form cross-β fibrils under mild conditions [13]. This study proposed that conformational strain present in the w.t. β2m DE loop, indicated by the left-handed α-helix conformation that Trp60 adopts in the MHC-I complex, would be released by the Trp60 → Gly mutation. Moreover, while residue Trp60 is stabilised in a low polarity niche on the surface of the heavy chain in the MHC-I complex, it is completely solvent exposed, thus potentially destabilizing, when β2m is dissociated from the heavy chain; a smaller, or more polar residue would therefore better fit this site in the isolated β2m chain.

The W60C crystal structure shows that the DE loop adopts the same regular β-turn conformation observed in W60G. However, although at lower efficiency relative to the w.t., W60C forms fibrils under mild conditions, a property not shared by W60G. Hence, apparently, a regular β-turn conformation in the DE loop is not the (only) structural determinant accounting for the lower propensity to fibril formation displayed by W60G. On the other hand, thermal unfolding shows that W60C and w.t. β2m display very similar Tm values, 59.8 and 60.1 °C, respectively. So, W60C, while having a structure of the DE loop that differs markedly from that of the isolated w.t. protein, displays properties grossly similar to w.t. β2m for what concerns stability and fibrillogenesis. These results suggest that such properties cannot be properly rationalized based on the static structures achieved by the DE loop (*i.e.* the starting protein conformation), nor on the Trp/Cys nature of residue 60. The decreased fibrillogenic propensity of W60G [13], however, suggests that the conformational freedom coded by Gly at site 60 is a key structural factor playing a regulatory role in β2m fibril aggregation, adding to the putative dependence of β2m fibrillogenesis on the physico-chemical properties of the DE region suggested by Platt et al. [26].

Based on the results achieved for W60G and W60C, it was deemed relevant to design a mutant (D59P) that would increase rigidity of the DE loop, since this should have a visible effect on β2m stability and fibrillogenesis. The D59P crystal structure shows evidence of backbone conformational strain in the mutated region, as indicated by deviation from planarity of Pro59 peptide ω angle, and by the Ramachandran outlier character of Ser57. Thermal unfolding of D59P shows a Tm drop of about 8 °C relative to w.t. β2m, indicating a significant loss in overall protein stability. Accordingly, relative to the w.t. protein, D59P displays an increased propensity to aggregate into fibrils, forming amyloid precipitate more quickly and yielding higher amounts of fibrillar aggregates.

The results here reported indicate that as long as a Cβ atom is present at residue 60, the thermal stability and the aggregation properties of β2m are affected only marginally, whereas large stability and fibrillation changes are associated with the W60G mutation. These observations suggest that complex phenomena, not directly observable in the crystal structures of the natively folded

protein, regulate fibril aggregation of the β2m site-60 mutants, in keeping with the suggestion that residue 60 is directly involved in stabilization of the assembled fibrils [11,27]. On the other hand, since the Asp → Pro mutation increases the rigidity of the DE loop at the expenses of some strain, lower thermal stability and an associated stronger tendency to amyloid aggregation can be rationalized based on the D59P structure.

Acknowledgments

This work was supported by the Italian Ministry of Education, University and Research (PRIN and FIRB projects RBNE03PX83, RBLA03B3KC_005), by Fondazione Cariplo (Progetto Nobel), by the European Union EURAMY Project, by Progetto Regione Lombardia, and by Ricerca Finalizzata Malattie Rare (Italian Ministry of Health).

References

[1] G. Merlini, V. Bellotti, Molecular mechanisms of amyloidosis, N. Engl. J. Med. 349 (2003) 583–596.
[2] R. Nelson, D. Eisenberg, Structural models of amyloid-like fibrils, Adv. Protein Chem. 73 (2006) 235–282.
[3] M. Sunde, L.C. Serpell, M. Bartlam, P.E. Fraser, M.B. Pepys, C.C. Blake, Common core structure of amyloid fibrils by synchrotron X-ray diffraction, J. Mol. Biol. 273 (1997) 729–739.
[4] S.A. Porcelli, R.L. Modlin, The CD1 system: antigen-presenting molecules for T cell recognition of lipids and glycolipids, Annu. Rev. Immunol. 17 (1999) 297–329.
[5] P.J. Bjorkman, M.A. Saper, B. Samraoui, W.S. Bennett, J.L. Strominger, D.C. Wiley, Structure of the human class I histocompatibility antigen, HLA-A2, Nature 329 (1987) 506–512.
[6] F. Gejyo, T. Yamada, S. Odani, Y. Nakagawa, M. Arakawa, T. Kunitomo, H. Kataoka, M. Suzuki, Y. Hirasawa, T. Shirahama, et al., A new form of amyloid protein associated with chronic hemodialysis was identified as beta 2-microglobulin, Biochem. Biophys. Res. Commun. 129 (1985) 701–706.
[7] N.M. Kad, S.L. Myers, D.P. Smith, D.A. Smith, S.E. Radford, N.H. Thomson, Hierarchical assembly of beta2-microglobulin amyloid in vitro revealed by atomic force microscopy, J. Mol. Biol. 330 (2003) 785–797.
[8] V. Bellotti, M. Stoppini, P. Mangione, M. Sunde, C. Robinson, L. Asti, D. Brancaccio, G. Ferri, Beta2-microglobulin can be refolded into a native state from ex vivo amyloid fibrils, Eur. J. Biochem. 258 (1998) 61–67.
[9] G. Esposito, R. Michelutti, G. Verdone, P. Viglino, H. Hernandez, C.V. Robinson, A. Amoresano, F. Dal Piaz, M. Monti, P. Pucci, P. Mangione, M. Stoppini, G. Merlini, G. Ferri, V. Bellotti, Removal of the N-terminal hexapeptide from human beta2-microglobulin facilitates protein aggregation and fibril formation, Protein Sci. 9 (2000) 831–845.
[10] E. Chatani, Y. Goto, Structural stability of amyloid fibrils of beta(2)-microglobulin in comparison with its native fold, Biochim. Biophys. Acta 1753 (2005) 64–75.
[11] M. Kihara, E. Chatani, K. Iwata, K. Yamamoto, T. Matsuura, A. Nakagawa, H. Naiki, Y. Goto, Conformation of amyloid fibrils of beta2-microglobulin probed by tryptophan mutagenesis, J. Biol. Chem. 281 (2006) 31061–31069.
[12] M. Hoshino, H. Katou, Y. Hagihara, K. Hasegawa, H. Naiki, Y. Goto, Mapping the core of the beta(2)-microglobulin amyloid fibril by H/D exchange, Nat. Struct. Biol. 9 (2002) 332–336.
[13] G. Esposito, S. Ricagno, A. Corazza, E. Rennella, D. Gumral, M.C. Mimmi, E. Betto, C.E. Pucillo, F. Fogolari, P. Viglino, S. Raimondi, S. Giorgetti, B. Bolognesi, G. Merlini, M. Stoppini, M. Bolognesi, V. Bellotti, The controlling roles of Trp60 and Trp95 in beta2-microglobulin function, folding and amyloid aggregation properties, J. Mol. Biol. 378 (2008) 885–895.
[14] CCP4, The CCP4 suite: programs for protein crystallography, Acta Crystallogr. D Biol. Crystallogr. 50 (1994) 760–763.
[15] A.G.W. Leslie, Recent changes to the MOSFLM package for processing film and image plate data, Joint CCP4 + ESF-EACMB Newsletter on Protein Crystallography 26 (1992).
[16] A.J. McCoy, R.W. Grosse-Kunstleve, P.D. Adams, M.D. Winn, L.C. Storoni, R.J. Read, Phaser crystallographic software, J. Appl. Cryst. 40 (2007) 658–674.
[17] G.N. Murshudov, A.A. Vagin, E.J. Dodson, Refinement of macromolecular structures by the maximum-likelihood method, Acta Crystallogr. D Biol. Crystallogr. 53 (1997) 240–255.
[18] P. Emsley, K. Cowtan, Coot: model-building tools for molecular graphics, Acta Crystallogr. D Biol. Crystallogr. 60 (2004) 2126–2132.
[19] U.B. Ericsson, B.M. Hallberg, G.T. Detitta, N. Dekker, P. Nordlund, Thermofluor-based high-throughput stability optimization of proteins for structural studies, Anal. Biochem. 357 (2006) 289–298.
[20] S. Yamamoto, I. Yamaguchi, K. Hasegawa, S. Tsutsumi, Y. Goto, F. Gejyo, H. Naiki, Glycosaminoglycans enhance the trifluoroethanol-induced extension of beta 2-microglobulin-related amyloid fibrils at a neutral pH, J. Am. Soc. Nephrol. 15 (2004) 126–133.
[21] H. Naiki, N. Haschimoto, S. Suzuki, H. Rimura, K. Nakakuki, F. Gejyo, Establishment of a kinetic model of dialysis-related amyloid fibril extension in vitro. AMYLOID, Int. Exp. Clin. Invest. 4 (1997) 223–232.
[22] H. LeVine 3rd., Thioflavine T interaction with synthetic Alzheimer's disease beta-amyloid peptides: detection of amyloid aggregation in solution, Protein Sci. 2 (1993) 404–410.
[23] C.H. Trinh, D.P. Smith, A.P. Kalverda, S.E. Phillips, S.E. Radford, Crystal structure of monomeric human beta-2-microglobulin reveals clues to its amyloidogenic properties, Proc. Natl. Acad. Sci. USA 99 (2002) 9771–9776.
[24] F. Fogolari, A. Corazza, P. Viglino, P. Zuccato, L. Pieri, P. Faccioli, V. Bellotti, G. Esposito, Molecular dynamics simulation suggests possible interaction patterns at early steps of {beta}2-microglobulin aggregation, Biophys. J. 92 (2007) 1673–1681.
[25] A. Relini, S. De Stefano, S. Torrassa, O. Cavalleri, R. Rolandi, A. Gliozzi, S. Giorgetti, S. Raimondi, L. Marchese, L. Verga, A. Rossi, M. Stoppini, V. Bellotti, Heparin strongly enhances the formation of beta2-microglobulin amyloid fibrils in the presence of type I collagen, J. Biol. Chem. 283 (2008) 4912–4920.
[26] G.W. Platt, K.E. Routledge, S.W. Homans, S.E. Radford, Fibril growth kinetics reveal a region of beta2-microglobulin important for nucleation and elongation of aggregation, J. Mol. Biol. 378 (2008) 251–263.
[27] F. Bemporad, N. Taddei, M. Stefani, F. Chiti, Assessing the role of aromatic residues in the amyloid aggregation of human muscle, Protein Sci. 15 (2006) 862–870.